Journal of Hazardous Materials 192 (2011) 1314–1320

Contents lists available at ScienceDirect

Journal of Hazardous Materials

journal homepage: www.elsevier.com/locate/jhazmat

Anatase–brookite mixed phase nano TiO_2 catalyzed homolytic decomposition of ammonium nitrate

Anuj A. Vargeese*, Krishnamurthi Muralidharan

School of Chemistry and Advanced Centre of Research in High Energy Materials, University of Hyderabad, Hyderabad 500046, India

ARTICLE INFO

Article history:
Received 6 April 2011
Received in revised form 11 June 2011
Accepted 14 June 2011
Available online 13 July 2011

Keywords:
Nano titanium dioxide
Catalysis
Structure-property relationships
Ammonium nitrate
Isoconversional kinetics

ABSTRACT

Compared to the conventional ammonium perchlorate based solid rocket propellants, burning of ammonium nitrate (AN) based propellants produce environmentally innocuous combustion gases. Application of AN as propellant oxidizer is restricted due to low reactivity and low energetics besides its near room temperature polymorphic phase transition. In the present study, anatase–brookite mixed phase TiO_2 nanoparticles (~10 nm) are synthesized and used as catalyst to enhance the reactivity of the environmental friendly propellant oxidizer ammonium nitrate. The activation energy required for the decomposition reactions, computed by differential and non-linear integral isoconversional methods are used to establish the catalytic activity. Presumably, the removal of NH_3 and H_2O, known inhibitors of ammonium nitrate decomposition reaction, due to the surface reactions on active surface of TiO_2 changes the decomposition pathway and thereby the reactivity.

© 2011 Elsevier B.V. All rights reserved.

1. Introduction

The application of nanoparticles has extended to almost all conceivable field of science ranging from medicine to rocketry. Even though, the nano-scale technology is multifaceted in its application, the use of nanoparticles as catalysts is perhaps the most captivating. Good catalytic activity of transition metal oxides (TMO) is attributed to their partially filled penultimate *d* orbitals and the subsequent binding sites provided to the intermediates formed during the reaction. The applications of TMO in industrial process as well as in thermal decomposition reactions are long known [1–3]. Moreover, the addition of TMO is known to improve the performance of solid propellants [4]. Hence, there is an interest in understanding the mechanism of action of TMO catalysts on the decomposition of propellants and its major ingredients such as oxidizer. The catalytic property evaluation of transition metal oxides, Fe_2O_3, CuO, Cu_2O, ZnO, CdO, NiO, TiO_2 and VO_2, both in micro and nano size on the decomposition and combustion of ammonium perchlorate and ammonium perchlorate based propellant systems are commonly found in literature [5–7].

Environmental effects of the exhaust products of conventional ammonium perchlorate based rocket propellants have been assessed by different investigators [8]. Areas of concern have included stratospheric ozone, acid rain, toxicity, air quality and global warming. Since then, there is an increased interest in research and development of eco-friendly solid propellant systems. Irrespective of its drawbacks, such as phase transitions, low performance and low burning rate, ammonium nitrate (AN) is receiving a reinvigorated interest as a possible substitute for ammonium perchlorate, due to eco-friendly plumes, smokelessness and low sensitivity [9,10].

One of the main drawbacks which restrict the application of AN as propellant oxidizer is its low reactivity and low energetics. Since TMOs are good catalyst for thermal decomposition reactions, increased reactivity of AN can be achieved by nano sized TMOs. Consequently, the interest in understanding and evaluating the effect of TMOs in the ultrafine particle form has attracted wide attention [11]. The competence of TiO_2, in micro as well as nano size, is well demonstrated in fields varying from photocatalysis to fuel cell applications. Even though, nano TiO_2 (NT) is an intensely studied material for catalytic applications [12,13], the investigations on the application of this material in tailoring energetic reactions are restricted to a few [11]. In Particular, the effect and application of TMO nanoparticles as catalyst for the decomposition reactions of AN still remains unexplored. Even if, a substantial increase in reactivity of the chemical decomposition reactions by nanocatalyst assistance might be anticipated, such decompositions are often dependent on the material property of the nanoparticles. The material property of the nanocomponents, which can influence the catalytic efficiency and possible reaction

* Corresponding author. Tel.: +91 40 66794919; fax: +91 40 23012460.
E-mail address: dr_anuj@ymail.com (A.A. Vargeese).

0304-3894/$ – see front matter © 2011 Elsevier B.V. All rights reserved.
doi:10.1016/j.jhazmat.2011.06.036

pathways could be surface area, shape, spatial distribution, surface composition, electronic structure, thermal and chemical stability, etc. [14].

It is widely considered that the catalysts which accelerate the oxidizer decomposition enhance the burning rate of propellant, but there is no well established proof for the argument. The catalytic effect of TMO on the thermal decomposition may be attributed to many reasons, such as semiconductor properties (degree of *p* or *n* nature), charge transfer process or electron transfer process, but the actual mechanism of activity still not known to any certainty. The *p* type semiconduction nature of oxides is reportedly contributory in enhancing the reactivity [3]. Earlier investigators report a linear dependency between the degree of catalytic activity of TMO on propellants with their redox potentials and the heat of reaction with the electron transfer process [4]. In the present study, the catalytic activity of NT on the AN decomposition behaviour/reaction was evaluated. Anatase–brookite mixed phase TiO_2 nanoparticles were synthesized by sol–gel method, via hydrolysis and peptization of titanium isopropoxide solution and used as the nanocatalyst to enhance the thermal decomposition rate of AN. The catalytic activity and efficiency of NT was estimated by computing the energy of activation values of AN and AN in presence of varying weight percentage of NT. For kinetic computations, two different isoconversional methods, Friedman's differential [15] and Vyazovkin's non-linear integral [16] methods, employing a series of non-isothermal experiments, were used. The normalized heat of decomposition (ΔH_d) of AN and AN–NT mixture were evaluated and compared to ascertain any change in heat of reaction. These analyses were used to establish the catalytic activity and assistance of NT on the decomposition reaction of AN.

2. Material and methods

2.1. Synthesis of nano TiO_2 nanocatalyst

Most TiO_2 synthesis route involves the use of titanium alkoxide or titanium chloride as precursor [17–20]. In the present study, NT with uniform size was synthesized by the hydrolysis of titanium isopropoxide solution. The procedure in brief, 250 mL deionized water was taken in a beaker and the pH of the solution was adjusted to 2 using dilute HNO_3 solution. 5 mL titanium isopropoxide was added to 15 mL of isopropyl alcohol, mixed vigorously, and then added drop wise to the pH adjusted deionized water with stirring (at 200 rpm). After 10 min, the stirring speed was reduced to 50 rpm and evaporated over a hot plate while the temperature of the reaction mixture was maintained at 80 °C. The evaporation was continued till the volume of the reaction mixture was reduced to ~25 mL (~18 h) and then it was transferred to a hot air oven maintained at 100 °C. After 3 h heating, an off-white solid of TiO_2 nanoparticles was collected. The solid was washed with ethanol and then heated at 200 °C for 3 h (as per TG-DT analysis) and then used for further experiments. The NT was characterized by PXRD, TEM and TG-DTA.

2.2. Preparation of AN–NT mixture

AN–NT mixtures with varying weight percentage of NT content viz., 0.5, 1 and 2% (referred as AT0.5, AT1 and AT2) were prepared by blending on a mechanical stirrer for 12 h. Crushed and sieved particles in the size of 105–180 μm of AN was used for the experiments. Since the molecular weight of AN and TiO_2 are very close by, the percentage values can be directly considered as molar ratios. After preparation the mixture was dried over fused calcium chloride under reduced pressure for 30 min. The dried mixture was used for catalytic activity evaluation and decomposition kinetic analysis.

2.3. Thermal analysis

Thermogravimetric analysis (TGA) measurements were carried out on a Mettler–Toledo TGA/DSC 1 instrument. In all experiments ~1 mg of samples was loaded in open 90 μL alumina pans and heated. Nitrogen at a flow rate of 30 mL/min was used as the purge and protective gas.

2.4. TEM analysis

The HRTEM study was carried out on a FEI Tecnai G^2 F20 S-Twin Transmission Electron Microscope. The samples for TEM and HRTEM analyses were obtained by diluting the dispersed solution with ethanol and then placing a drop of the diluted solution onto a Formvar covered copper grid and evaporated in air at room temperature.

2.5. Powder XRD

The powder X-ray diffraction (PXRD) patterns were obtained using a 'Bruker D8 Advance' instruments at room temperature (25 °C) and the sample was scanned over a 2θ range of 10–70°. A step size or sampling interval of 0.001° and a scan time of 7.6 s was used for the characterization. From the obtained PXRD patterns, the interplanar distances (d) were calculated by Bragg's equation and compared with the JCPDS data.

2.6. Decomposition kinetic analysis

Thermogravimetric analysis (TGA) measurements were used to determine the decomposition kinetics of the samples. Non-isothermal TGA runs were conducted at heating rates 2.5, 5, 10 and 20 °C/min and the extend of conversion (α) has been computed from the weight loss data using the reported standard method [21]. $\Delta\alpha$ of 0.01 and a $\Delta\alpha$ of 0.025 were respectively used to compute the activation energy (E_α) from the differential and the integral methods. For comparison and plotting, constant α values were shown at an interval of 0.05.

2.7. Friedman (differential) method

The differential isoconversional method of Friedman [15] is based on the Arrhenius Eq. (1).

$$\frac{d\alpha}{dt} = A\ \exp\left(-\frac{E}{RT}\right) f(\alpha) \tag{1}$$

Friedman analysis applies the logarithm of the conversion rate $d\alpha/dt$ as a function of the reciprocal temperature at different degrees of the conversion α. This modification results in Eq. (2)

$$\ln\left(\frac{d\alpha}{dt}\right)_{\alpha,i} = \ln\left[A_\alpha f(\alpha)\right] - \left(\frac{E_\alpha}{RT_{\alpha,i}}\right) \tag{2}$$

Hence by plotting $\ln(d\alpha/dt)$ versus $1/T$ at constant α values a family of straight lines with slope $-E_\alpha/R$ is obtained. Similar way the activation energy of AN and AN–NT mixtures was computed.

2.7.1. Vyazovkin (non-linear integral) method

Vyazovkin method is a non-linear integral isoconversional method which can be used for non-isothermal experiments. Vyazovkin method provides more precise activation energy values by performing numerical integration [16]. For a set of n experiments carried out at different heating rates, the activation energy can be determined at any particular value of α by finding the value of E_α for which the given function, Eq. (3), is a minimum. The minimization

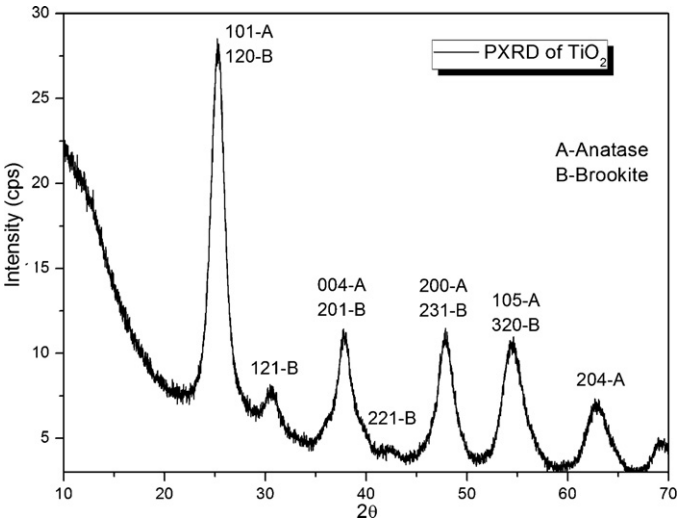

Fig. 1. PXRD pattern of anatase–brookite mixed phase nano TiO_2.

procedure is repeated for each value of α to find the dependency of the activation energy on the extent of conversion.

$$\sum_{i}^{n}\sum_{j\neq i}^{n}\left[I(E_\alpha, T_{\alpha,i})\beta_j\right] / \left[I(E_\alpha, T_{\alpha,j})\beta_i\right] = \min \quad (3)$$

$$\text{where} \quad I(E,T) = \int_0^T \exp\left(-\frac{E}{RT}\right) \mathrm{d}T \quad (4)$$

β in Eq. (3) denotes the heating rates and the indexes i and j denote set of experiments performed under different heating rates and n is the total number of experiments performed.

The third degree approximation (Eq. (6)) proposed by Senum and Yang [22] has been used in the present study to evaluate the integral Eq. (4).

$$I(E,T) = \frac{E}{R}f(x) \quad (5)$$

$$\text{where} \quad f(x) = \frac{\exp(-x)}{x} \times \frac{x^2+10x+18}{x^3+12x^2+36x+24} \quad (6)$$

$$\text{and} \quad x = \frac{E}{RT} \quad (7)$$

MATLAB 7.0.1 was used to perform the kinetic computations.

3. Results and discussion

3.1. Synthesis and structural characterizations of TiO_2 nanocatalyst

A mixture of titanium isopropoxide and isopropyl alcohol was used to synthesize the NT. The formation of NT is explained as follows, the pH of the hydrolysis solution was adjusted to 2 and in the high acidic medium, because of the polarizability of Ti^{4+} ions, different complexes with varying valances are formed. The oxolation and olation process occurs simultaneously during nucleation and further leads to the precipitation of hydrous oxide [23]. Heating the solution (thermolysis process) promotes these reactions and in turn the precipitation of NT.

The PXRD pattern of the NT was obtained as described in the experimental section and is shown in Fig. 1. Examination of the PXRD pattern indicated two possibilities, either the formation of TiO_2 brookite phase or a mixture of brookite and anatase phase. The 100% intensity peak of rutile (1 1 0) was not observed in the pattern

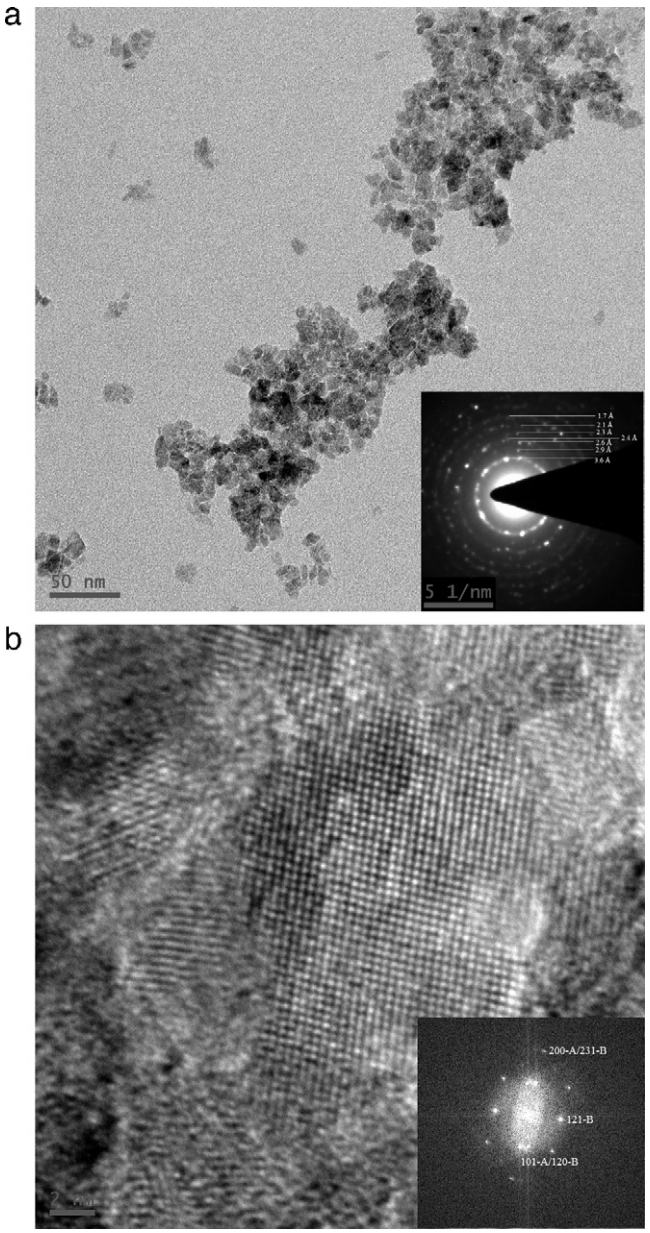

Fig. 2. Nanosized TiO_2 (a) TEM image with Electron Diffraction pattern inset (b) HRTEM image with corresponding FFT inset.

and hence its presence was ruled out. Formation of agglomerates of nanosized particles was indicated by the broadness of the X-ray diffraction lines. Even though the hydrolysis of titanium isopropoxide reportedly leads to the formation of TiO_2 anatase phase [24], sol–gel synthesis of titania typically produces a mixture of brookite and anatase [25]. The presence of brookite phase was clearly evident from the well distinguished peaks corresponding to $h\,k\,l$ values 1 2 1 and 2 2 1. The 100% intensity (1 0 1) peak of anatase and the 100% intensity (1 2 0) and 80% intensity (1 1 1) peaks of brookite are very nearby (JCPDS 21-1272 and 29-1360). Since anisotropic peak broadening, related to crystallite shape, defects, and microstrain, occur in nanomaterials, these higher intensity peaks may overlap. The peak overlap of anatase and brookite phases has been reported by earlier investigators and suggests numeric deconvolution technique to separate these peaks [26]. Since such a study does not fall in the perspective of this work and well distinguished higher intensity peaks of anatase (2 0 4) and brookite (1 2 1) were iden-

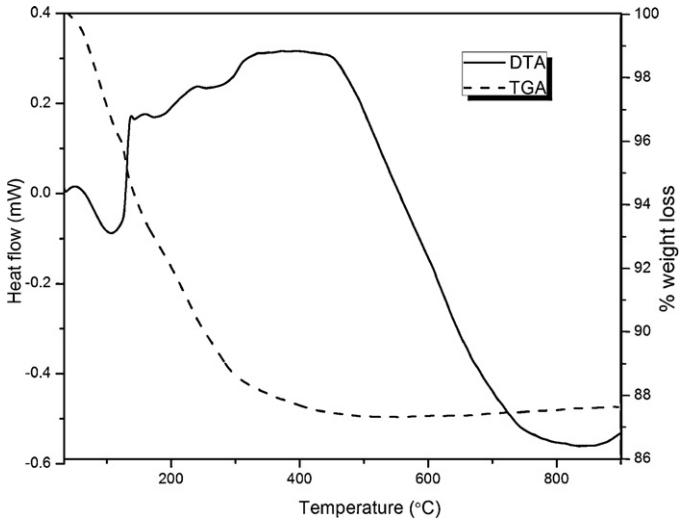

Fig. 3. TG-DTA of nanosized TiO_2.

tified, the obtained NT is considered as a mixture of brookite and anatase phase. The brookite phase content of the mixture, from the PXRD peak intensities, can be estimated to be about 25% or probably slightly more.

TEM images, shown in Fig. 2, were used to investigate the particle size, crystallinity and morphology of the synthesized NT. The TEM micrograph shows a relatively narrow size distribution of nanoparticles with a mean particle diameter of 10 nm. However, the TEM also illustrates the presence of small aggregates of TiO_2 with diameter ~50 nm. Observations in several zones show that most of the particles crystallize in platelet morphology with positive and negative curvature. The high resolution TEM image shows lattice fringes related to the crystal structure of the particles. The electron diffraction pattern exhibited the presence of both anatase and brookite phase with two characteristic diffraction rings (1 2 1 and 2 2 1) corresponding to the brookite phase. Hence, the electron diffraction data is in good agreement with the PXRD observations.

To confirm the chemical composition, TG-DT analysis of the NT was performed. The measured curve (Fig. 3) indicated a total weight loss of ~12% below 375 °C in the exposed temperature range 30–900 °C. The initial weight loss at ~100 °C is associated with an endothermic peak, which shows the dehydration of $TiO_2 \cdot H_2O$ as well as the removal of surface attached H_2O due to physisorbtion. Approximately 4% of the weight loss can be attributed to the H_2O removal. The remaining 8% weight loss is due to the removal of organic impurities crystallized along with the particles. At around 375 °C, the weight becomes constant indicating complete removal of organic impurities. Furthermore, no endothermic peak was observed suggesting any crystallographic phase transition occurred in the temperature region in which the compound was exposed [27]. Since approximately 70% of the total weight loss occurs before 200 °C, the sample was annealed at this temperature for 3 h before evaluating the catalytic efficiency.

3.2. Catalytic decomposition of ammonium nitrate

AN–NT mixtures with NT content viz., 0.5, 1 and 2% were prepared by physical mixing. The TG-DTA curves measured at 10 °C/min heating rate, shown in Fig. 4, were used to study the decomposition temperature and thermal stability of the samples. The measured curves clearly indicate a shift in the decomposition temperature corresponding to the concentration of the nanocatalyst. The peak decomposition temperature observed and the ΔH_d values are tabulated in Table 1. Also, in the DTA thermogram, the melting peak is influenced by the presence of nanocatalyst, probably behaving as an impurity, causing a decrease in the melting point. These observations were invariably similar in the data obtained at different heating rates.

In addition, the ΔH_d values of the samples obtained were compared. Surprisingly, the endothermicity of the AN decomposition was significantly brought down, i.e., the decomposition reaction became more exothermic in nature with respect to the catalyst concentration. Since, the enhancement of heat of reaction by catalyst assistance is thermodynamically incorrect, the possible reason may be a change in the reaction pathway. In view of the fact that, a variety of decomposition reaction pathways that AN can undergo and are (except proton transfer reaction) exothermic in nature [28], the possibility of a change in the reaction pathway due to the catalyst assistance is more likely indicated as a change in ΔH_d.

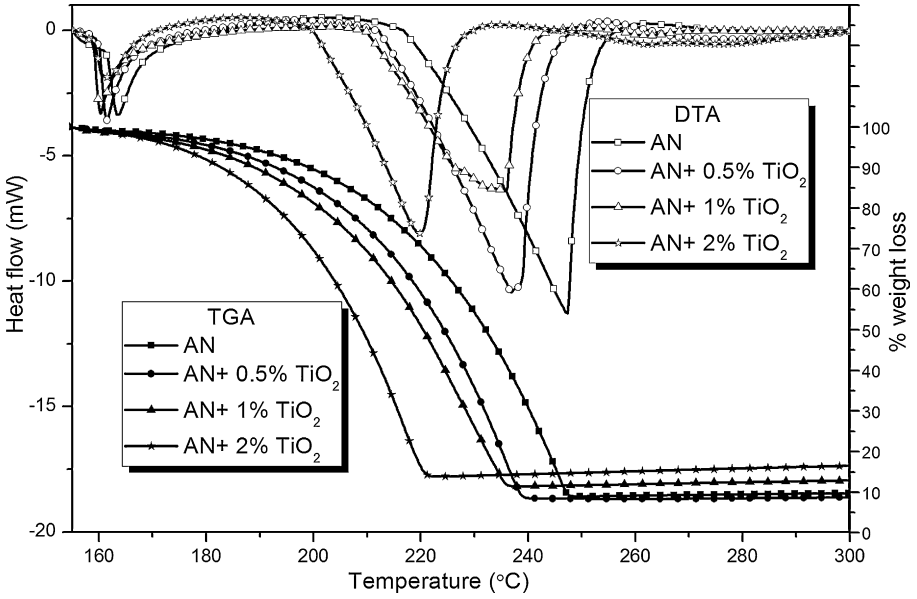

Fig. 4. TG-DTA of AN–NT mixtures obtained at 10 °C/min.

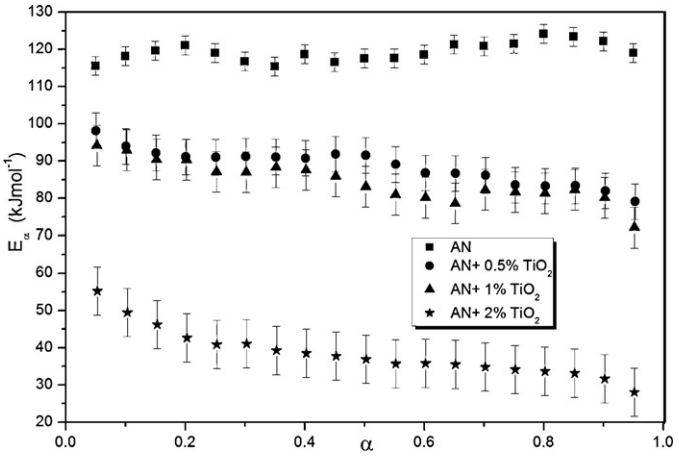

Fig. 5. E_α dependency on α computed by Friedman method.

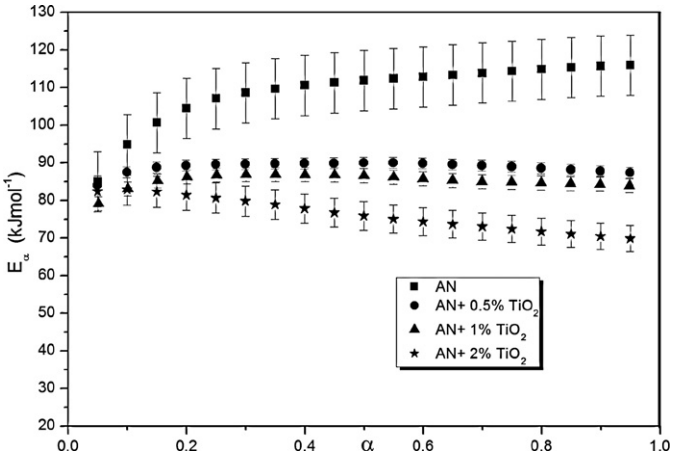

Fig. 6. E_α dependency on α computed by Vyazovkin method.

The calculated activation energy (E_α) values of the decomposition reaction of AN were plotted against extend of conversion (α) and shown in Figs. 5 and 6. Activation energy may be correlated to bond energy data [29] and is generally considered as a measurement of the energy barrier to a controlling (rate limiting) bond rupture or bond redistribution step [30]. The activation energy can provide reasonable information about critical energy needed to start the decomposition reaction of the compound. Hence, a reduction in the activation energy can be directly correlated to the catalytic activity of the compounds under investigation.

It is well accepted by the previous researchers that the overall decomposition reaction of AN is described by the first order reaction kinetics, but the reported values of activation energy for the process varies from 86.2 to 206.9 kJ mol^{-1} [31,32]. A recent work reports the thermal gasification of AN has a similar kinetics in the solid and liquid phase and requires an activation energy of ~90 kJ mol^{-1} [33]. A reaction system following first order reaction kinetics (or unification of multiple-reaction mechanisms) can be identified from the independent relation between E_α and α, which remains true for AN in the present study.

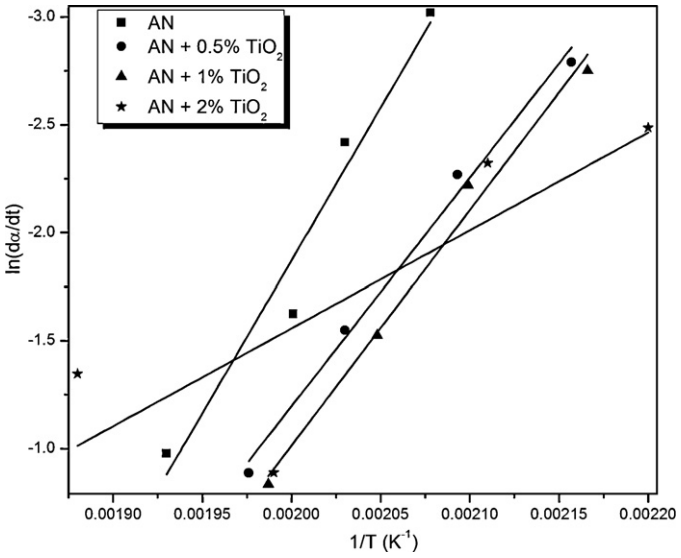

Fig. 7. Isoconversional Arrhenius plots based on Freidman's method at $\alpha = 0.4$.

$$NH_4NO_3 \longrightarrow NH_3 + HNO_3$$

Scheme 1. Thermal dissociation of ammonium nitrate.

For all the catalyzed reactions a significant reduction in the activation energy was observed. The plots of E_α against α of AT2 indicate a change in the decomposition reaction pathway besides a significant reduction in the E_α values. In other words, instead of the earlier reported first order reaction kinetics and a linear relation, the E_α value of AT2 varies significantly as the reaction proceeds. The E_α and α plot obtained using Friedman's method, especially of AT2, show a gradual decrease in the E_α values strongly indicating the catalytic activity. More precisely, the isoconversional Arrhenius plots at $\alpha = 0.4$ shown in Fig. 7 illustrates a substantial slope difference for the mixtures and a corresponding change in the E_α values. The variation in activation energy could occur due to the heterogeneous nature of the solid sample or due to a complex reaction mechanism. Two or more elementary steps, with independent activation energy can also affect the rate of reaction.

Even though all the mixtures showed a change in the reaction pathway, resultant to the percentage of the catalyst, the decomposition pathway of AT0.5 and AT1 did not show a noticeable difference as in the case of AT2. This could be considered as an indication of the minimum catalyst quantity required to significantly influence the reaction pathway. The non-linear relation of E_α with α for AT2 can be explained with respect to the thermal decomposition of AN. The thermal decomposition reaction of AN can occur in a variety of pathways, but the reaction is initiated by an endothermic proton transfer reaction (Scheme 1) [28]. Considering the fact that the DTA thermogram exhibited endothermic nature of the decomposition, and all other reported decomposi-

Table 1
Decomposition data of AN and AN–TiO_2 mixtures at heating rate 10 °C/min.

Ammonium nitrate (%)	Catalyst TiO_2 (%)	Peak decomposition temperature (°C)	Heat of decomposition (normalized) (Jg^{-1})	E_α by Friedman method (kJ mol^{-1})	E_α by Vyazovkin method (kJ mol^{-1})
100	0	247	−803	119 (±2.5)	109 (±8)
99.5	0.5	240	−614	88 (±4.7)	89 (±1.4)
99	1	236	−583	84 (±5.4)	85 (±1.8)
98	2	221	−523	38 (±6.4)	76 (±4.3)

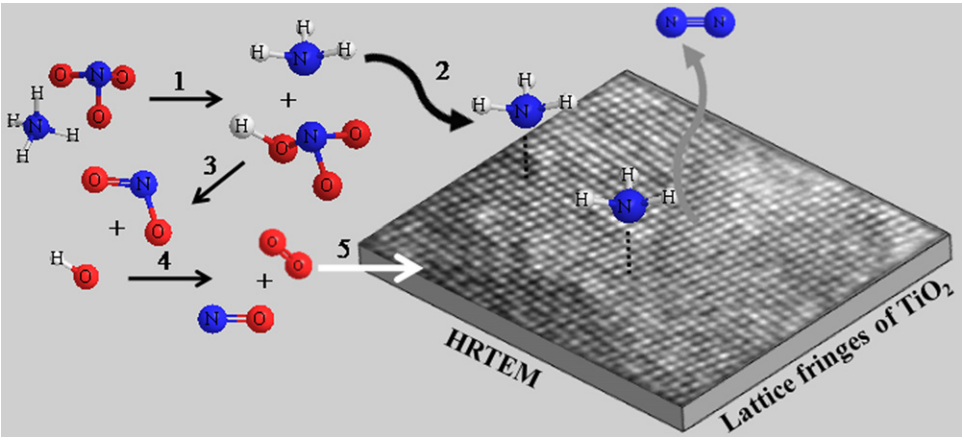

Fig. 8. Mechanism of catalytic decomposition of ammonium nitrate.

a) $NH_3 \longrightarrow NH_2 + H$
b) $2NH_2 \longrightarrow N_2H_4$
c) $N_2H_4 \longrightarrow N_2 + 4H$
d) $4H + O_2 \longrightarrow 2H_2O$

Scheme 2. Surface reactions after NH_3 adsorption.

a) $HNO_3 \longrightarrow OH + NO_2$
b) $NO_2 \longrightarrow NO + 1/2O_2$

Scheme 3. Decomposition of ammonium nitrate dissociation products.

tion pathways are exothermic in nature, the possibility of reaction shown in Scheme 1 seems apparent in the present system. In the non-catalyzed AN decomposition, the dissociation product HNO_3 further dissociates and reacts with NH_3 to form N_2O and H_2O [28].

The interaction between TiO_2, especially of anatase phase, and ammonia is well established by different investigators [34]. TiO_2 exhibits reasonable catalytic activity in the oxidation of ammonia to N_2 and N_2O in the temperatures below 300 °C [35]. The titanium atoms remaining after dehydroxylation are incompletely coordinated (and behave as Lewis acid centres) and can therefore fix either a water molecule or an ammonia molecule [36]. Hence, the NH_3 formed during the dissociation of AN may bond coordinatively to two different types of Lewis sites on the anatase surface. After adsorption, a surface reaction occurs in which hydrazine is formed as an intermediate. As shown below, the adsorbed NH_3 on the nanocatalyst give rise to N_2 through the decomposition of hydrazine produced by the dimerization of NH_2 species that is generated by the oxydehydrogenation (Scheme 2) [37,38].

The Oxygen required for the reaction could have produced due to the dissociation of NO_2 which in turn produced by the homolytic dissociation of HNO_3 (Scheme 3). The proposed reaction mechanism is schematically represented in Fig. 8. In the reaction mechanism, the reaction follows step (1) dissociation of ammonium nitrate, step (2) absorption of NH_3 on TiO_2 surface, step (3) dissociation of HNO_3 produced from ammonium nitrate, step (4) formed NO_2 further dissociates to NO and O_2, and step (5) O_2 interacts with TiO_2. The step 1, step 3 and step 4 are the reported thermal decomposition pathway of AN [39].

It has been demonstrated by earlier investigators that, NH_3 and H_2O inhibit the AN decomposition and on the other hand HNO_3 promotes the decomposition [39]. In the present study, the TiO_2 presumably removes the NH_3 from the system and hence the inhibitor concentration will be reduced as the reaction proceeds. The higher specific surface area of the NTs might facilitate higher adsorption of NH_3. The NH_3 removal process will perceptibly increase the rate of decomposition resulting in lesser E_α values. This change in the reaction path way appears to have altered the E_α with α relation and hence the kinetics. The variation of E_α values of a reaction during its progress can be attributed to a systematic change in the reaction kinetics. At lower concentration of NT, the active surface sites would have more rapidly inhibited by the higher concentration of NH_3, released from AN.

The activation energy required for the thermal decomposition of AN is 119 kJ mol^{-1} as per the differential method (or 109 kJ mol^{-1} as per the integral method), while that of AT0.5, AT1 and AT2 are 88, 84 and 38 kJ mol^{-1} (89, 85, and 76 kJ mol^{-1}), respectively. This shows that the numerical values of activation energy obtained by different isoconversional methods vary significantly. These differences could be due to the approximation of the temperature integral used in the isoconversional methods [40]. The differential method gives actual information of decomposition reaction while numerical integration suppresses this information. Most popular and conventional integral method of Flynn–Wall and Ozawa (linear integral method) has also been used for the comparison (supplementary data), which showed a similar trend and slightly higher numerical values than the non-linear integral method. Since Friedman's differential method uses the instantaneous rate values and sensitive to experimental noise, it gives larger variations in E_α dependency on conversion degree. Approximately, a difference of 20% in the absolute value of E_α obtained by differential and integral isoconversional methods is reported [41]. Hence, irrespective of the difference in numerical values the studies show a strong catalytic activity as well as a reaction pathway change in the NT assisted thermal decomposition of AN.

4. Conclusions

The catalytic efficiency of NT has been proved by demonstrating a significant reduction in the activation energy required for the NT assisted decomposition reaction of ammonium nitrate. At molar ratios (ammonium nitrate–TiO_2) as low as 49:1, the nanocatalyst changed the reactivity of ammonium nitrate decomposition by possibly altering the decomposition pathway. The activation energy values obtained by differential and non-linear integral methods showed similar reaction kinetics and E_α dependency on α. Probably the removal of ammonium nitrate decomposition reaction inhibition species, such as NH_3 on the TiO_2 surface and subsequent

oxidation leads to the change in the decomposition pathway. The findings of this work can be useful in realizing more environmentally benign solid propellant systems based on ammonium nitrate.

Acknowledgments

The authors thank Mija S.J. (NIT Calicut) for fruitful discussions and MATLAB code (for kinetic computations), DRDO for financial support to ACRHEM, Mr. A. Rajesh (CIL, University of Hyderabad) for collecting thermal analysis data, Centre for Nanotechnology, University of Hyderabad for providing the TEM facility and Mr. Durga Prasad Muvva for recording the TEM images. AAV acknowledges DST–UoH–PURSE (post doctoral) fellowship.

Appendix A. Supplementary data

Supplementary data associated with this article can be found, in the online version, at doi:10.1016/j.jhazmat.2011.06.036.

References

[1] M. Fujihira, Y. Satoh, T. Osa, Heterogeneous photocatalytic oxidation of aromatic compounds on TiO_2, Nature 293 (1981) 206–208.
[2] G. Ramis, G. Busca, V. Lorenzelli, P. Forzatti, Fourier transform infrared study of the adsorption and coadsorption of nitric oxide, nitrogen dioxide and ammonia on TiO_2 anatase, Appl. Catal. 64 (1990) 243–257.
[3] W.K. Rudloff, E.S. Freeman, Catalytic effect of metal oxides on thermal decomposition reactions. II. Catalytic effect of metal oxides on the thermal decomposition of potassium chlorate and potassium perchlorate as detected by thermal analysis methods, J. Phys. Chem. 74 (1970) 3317–3324.
[4] K. Kishore, M.R. Sunitha, Mechanism of catalytic activity of transition metal oxides on solid propellant burning rate, Combust. Flame 33 (1978) 311–314.
[5] R.W. Armstrong, B. Baschung, D.W. Booth, M. Samirant, Enhanced propellant combustion with nanoparticles, Nano Lett. 3 (2003) 253–255.
[6] M.A. Stephens, E.L. Petersen, R. Carro, D.L. Reid, S. Seal, Multi-parameter study of nanoscale TiO_2 and CeO_2 additives in composite AP/HTPB solid propellants, Propellants Explos. Pyrotech. 35 (2010) 143–152.
[7] A. Gromov, Y. Strokova, A. Kabardin, A. Vorozhtsov, U. Teipel, Experimental study of the effect of metal nanopowders on the decomposition of HMX, AP and AN, Propellants Explos. Pyrotech. 34 (2009) 506–512.
[8] R.R. Bennett, J.R. Whimpey, R. Smith-Kent, A.J. McDonald, Effects of rocket exhaust on the launch site environment and stratospheric ozone, Int. J. Energ. Mater. Chem. Prop. 4 (1997) 92–105.
[9] A.A. Vargeese, S.S. Joshi, V.N. Krishnamurthy, Effect of method of crystallization on the IV–III and IV–II polymorphic transitions of ammonium nitrate, J. Hazard. Mater. 161 (2009) 373–379, and references therein.
[10] A.A. Vargeese, S.S. Joshi, V.N. Krishnamurthy, Use of potassium ferrocyanide as habit modifier in the size reduction and phase modification of ammonium nitrate crystals in slurries, J. Hazard. Mater. 180 (2010) 583–589, and references therein.
[11] D.L. Reid, A.E. Russo, R.V. Carro, M.A. Stephens, A.R. LePage, T.C. Spalding, E.L. Petersen, S. Seal, Nanoscale additives tailor energetic materials, Nano Lett. 7 (2007) 2157–2161.
[12] U. Diebold, The surface science of titanium dioxide, Surf. Sci. Rep. 48 (2003) 53–229.
[13] C.-H. Ho, C.-Y. Shieh, C.-L. Tseng, Y.-K. Chen, J.-L. Lin, Decomposition pathways of glycolic acid on titanium dioxide, J. Catal. 261 (2009) 150–157.
[14] G.Q. Lu, X.S. Zhao, in: G.Q. Lu, X.S. Zhao (Eds.), Nanoporous Materials: Science and Engineering, Imperial College Press, London, 2004.
[15] H.L. Friedman, Kinetics of thermal degradation of char-forming plastics from thermogravimetry-application to a phenolic resin, J. Polym. Sci., Part C: Polym. Symp. 6 (1964) 183–195.
[16] S. Vyazovkin, Evaluation of activation energy of thermally stimulated solid-state reactions under arbitrary variation of temperature, J. Comput. Chem. 18 (1997) 393–402.
[17] L. Mao, Q. Li, H. Dang, Z. Zhang, Synthesis of nanocrystalline TiO_2 with high photoactivity and large specific surface area by sol–gel method, Mater. Res. Bull. 40 (2005) 201–208.
[18] T. Sugimoto, X. Zhou, A. Muramatsu, Synthesis of uniform anatase TiO_2 nanoparticles by gel–sol method: 1. solution chemistry of $Ti(OH)_n^{(4-n)+}$ complexes, J. Colloid Interface Sci. 252 (2002) 339–346.
[19] G. Oskam, A. Nellore, R.L. Penn, P.C. Searson, The growth kinetics of TiO_2 nanoparticles from titanium(iv) alkoxide at high water/titanium ratio, J. Phys. Chem. B 107 (2003) 1734–1738.
[20] N.-L. Wu1, S.-Y. Wang, I.A. Rusakova, Inhibition of crystallite growth in the sol-gel synthesis of nanocrystalline metal oxides, Science 285 (1999) 1375–1377.
[21] M.E. Brown, Introduction to Thermal Analysis: Techniques and Application, Kluwer Academic Publishers, New York, 2001.
[22] G.I. Senum, R.T. Yang, Rational approximations of the integral of the Arrhenius function, J. Therm. Anal. 11 (1977) 445–447.
[23] D. Dambournet, I.K. Belharouak, Amine, tailored preparation methods of TiO_2 anatase, rutile, brookite: mechanism of formation and electrochemical properties, Chem. Mater. 22 (2010) 1173–1179.
[24] S. Mahshid, M. Askari, M.S. Ghamsari, Synthesis of TiO_2 nanoparticles by hydrolysis and peptization of titanium isopropoxide solution, J. Mater. Process. Technol. 189 (2007) 296–300.
[25] S.L. Isley, R.L. Penn, Relative brookite and anatase content in sol–gel–synthesized titanium dioxide nanoparticles, J. Phys. Chem. B 110 (2006) 15134–15139.
[26] H. Zhang, J.F. Banfield, Understanding polymorphic phase transformation behavior during growth of nanocrystalline aggregates: insights from TiO_2, J. Phys. Chem. B 104 (2000) 3481–3487.
[27] K.N.P. Kumar, K. Keizer, A.J. Burggraaf, T. Okubo, H. Nagamoto, S. Morooka, Densification of nanostructured titania assisted by a phase transformation, Nature 358 (1992) 48–51.
[28] C. Oommen, S.R. Jain, Ammonium nitrate: a promising rocket propellant oxidizer, J. Hazard. Mater. 67 (1999) 253–281, and references therein.
[29] R. Schmid, V.N. Sapunov, Non-Formal Kinetics: In Search of Chemical Reaction Pathways, Verlag Chemie GmbH, Weinheim, 1982.
[30] A.K. Galwey, Is the science of thermal analysis kinetics based on solid foundations? A literature appraisal, Thermochim. Acta 413 (2004) 139–183.
[31] R. Gunawan, D. Zhang, Thermal stability and kinetics of decomposition of ammonium nitrate in the presence of pyrite, J. Hazard. Mater. 165 (2009) 751–758.
[32] A.G. Keenan, B. Dimitriades, Differential rate method for kinetic measurements. Thermal decomposition of ammonium nitrate, Trans. Faraday Soc. 57 (1961) 1019–1023.
[33] S. Vyazovkin, J.S. Clawson, C.A. Wight, Thermal dissociation kinetics of solid and liquid ammonium nitrate, Chem. Mater. 13 (2001) 960–966.
[34] J.M. Amores, V.S. Escribano, G. Ramis, G. Busca, An FT-IR study of ammonia adsorption and oxidation over anatase-supported metal oxides, Appl. Catal., B 13 (1997) 45–58.
[35] N.I. Il'chenko, Catalytic oxidation of ammonia, Russ. Chem. Rev. 45 (1976) 1119–1134.
[36] M. Primet, P. Pichat, M.V. Mathieu, Infrared study of the surface of titanium dioxides. II. Acidic and basic properties, J. Phys. Chem. 75 (1971) 1221–1226.
[37] C.C. Chuang, J.S. Shiu, J.L. Lin, Interaction of hydrazine and ammonia with TiO_2, Phys. Chem. Chem. Phys. 2 (2000) 2629–2633.
[38] J.G. Chang, S.P. Ju, C.S. Chang, H.T. Chen, Adsorption configuration and dissociative reaction of NH_3 on anatase (101) surface with and without hydroxyl groups, J. Phys. Chem. C 113 (2009) 6663–6672.
[39] K.R. Brower, J.C. Oxley, M. Tewari, J. Phys. Chem. 93 (1989) 4029–4033.
[40] B. Jankovic, B. Adnađevica, J. Jovanovica, Application of model-fitting and model-free kinetics to the study of non-isothermal dehydration of equilibrium swollen poly (acrylic acid) hydrogel: thermogravimetric analysis, Thermochim. Acta 452 (2007) 106–115.
[41] P. Budrugeac, D. Homentcovschi, E. Segal, Critical analysis of the isoconversional methods for evaluating the activation energy. II. The activation energy obtained from isothermal data corresponding to two successive reactions, J. Therm. Anal. Calorim. 63 (2001) 465–469.